2014

Annual patterns and budget of CO_2 flux in an Arctic tussock tundra ecosystem

Walter C. Oechel
San Diego State University

Cheryl A. Laskowski
San Diego State University

George Burba
LI-COR Biosciences, Lincoln, Nebraska, george.burba@licor.com

Beniamino Gioli
IBIMET CNR, Florence, Italy

Aram A. M. Kalhori
San Diego State University

AGU PUBLICATIONS

JGR

Journal of Geophysical Research: Biogeosciences

RESEARCH ARTICLE
10.1002/2013JG002431

Key Points:
- Showing patterns and vulnerabilities of CO_2 fluxes
- A change from an annual sink of CO_2 to an annual source
- To predict an estimate Arctic fluxes under future conditions

Correspondence to:
A. A. M. Kalhori,
akalhori@mail.sdsu.edu

Citation:
Oechel, W. C., C. A. Laskowski, G. Burba, B. Gioli, and A. A. M. Kalhori (2014), Annual patterns and budget of CO_2 flux in an Arctic tussock tundra ecosystem, *J. Geophys. Res. Biogeosci.*, *119*, 323–339, doi:10.1002/2013JG002431.

Received 28 JUN 2013
Accepted 25 JAN 2014
Accepted article online 4 FEB 2014
Published online 21 MAR 2014

Annual patterns and budget of CO_2 flux in an Arctic tussock tundra ecosystem

Walter C. Oechel[1,2], Cheryl A. Laskowski[1], George Burba[3], Beniamino Gioli[4], and Aram A. M. Kalhori[1]

[1]Global Change Research Group, San Diego State University, San Diego, California, USA, [2]Department of Geography, University of Leicester, Leicester, UK, [3]Research and Development, LI-COR Biosciences, Lincoln, Nebraska, USA, [4]Institute of Biometeorology, IBIMET CNR, Florence, Italy

Abstract The functioning of Arctic ecosystems is not only critically affected by climate change, but it also has the potential for major positive feedback on climate. There is, however, relatively little information on the role, patterns, and vulnerabilities of CO_2 fluxes during the nonsummer seasons in Arctic ecosystems. Presented here is a year-round study of CO_2 fluxes in an Alaskan Arctic tussock tundra ecosystem, and key environmental controls on these fluxes. Important controls on fluxes vary by season. This paper also presents a new empirical quantification of seasons in the Arctic based on net radiation. The fluxes were computed using standard FluxNet methodology and corrected using standard Webb-Pearman-Leuning density terms adjusted for influences of open-path instrument surface heating. The results showed that the nonsummer season comprises a significant source of carbon to the atmosphere. The summer period was a net sink of 24.3 g C m^{-2}, while the nonsummer seasons released 37.9 g C m^{-2}. This release is 1.6 times the summer uptake, resulting in a net annual source of +13.6 g C m^{-2} to the atmosphere. These findings support early observations of a change in this particular region of the Arctic from a long-term annual sink of CO_2 to an annual source from the terrestrial ecosystem and soils to the atmosphere. The results presented here demonstrate that nearly continuous observations may be required in order to accurately calculate the annual net ecosystem CO_2 exchange of Arctic ecosystems and to build predictive understanding that can be used to estimate, with confidence, Arctic fluxes under future conditions.

1. Introduction

The effect of the Arctic's carbon budget is a critical feedback on climate change. The Arctic contains over 2700 Gt of carbon as organic matter in the upper 3 m of soil and permafrost [*Schuur et al.*, 2008; *Lee et al.*, 2012], which represents over 43% of the global carbon content to this depth [*Tarnocai et al.*, 2009]. Much of this carbon has been sequestered since the beginning of the Holocene [*Zimov et al.*, 2009]. However, beginning in the mid-1970s, many Arctic soils have switched from a long-term sink to a source of CO_2 to the atmosphere, due to recent rapid warming and drying [*Gorham*, 1991; *Oechel et al.*, 1993, 2000; *Lund et al.*, 2012]. The Arctic may increase in source activity to the atmosphere. This is likely due to climatic change affecting Arctic ecosystems, including warming, soil drying, deepening of the active layer, and loss of permafrost [*Hinzman et al.*, 2005; *Natali et al.*, 2012], despite acclimatization and adjustments that may occur [*Oechel et al.*, 1993, 2000].

The net carbon budget of the Arctic is highly impacted by the very long "winter" season outside of the short Arctic growing season [*Groendahl et al.*, 2007; *Euskirchen et al.*, 2012]. This long nonsummer period of low or no vascular plant growth is increasingly recognized as a period of significant biological activity and large cumulative trace gas fluxes [*Zimov et al.*, 1993; *Oechel et al.*, 1997, 2000; *Panikov et al.*, 2006; *Marushchak et al.*, 2013]. The nonsummer period may be the dominant contribution to carbon-CO_2 flux in the Arctic [*Oechel et al.*, 1993; *Welker et al.*, 2000].

Our knowledge of the patterns and controls on nonsummer net CO_2 fluxes is still limited. There are a number of reasons for this including a slow realization of the large contribution of nonsummer periods to the annual trace gas budgets, in general [*McKane et al.*, 1997; *Oechel et al.*, 1997; *Fahnestock et al.*, 1999; *Welker et al.*, 2000; *Olsson et al.*, 2003; *Harazono et al.*, 2003; *Hirata et al.*, 2007], and the historic view that the bulk of biological activity occurs in the summer, such that the onset of winter leads to inactivity in the Arctic [*Oechel et al.*, 1995] also contributes to our limited knowledge. There has been a general underappreciation of how microbial and plant carbon fluxes at subzero temperatures [*Mastepanov et al.*, 2008] are impacted by: freeze-thaw events [*Grogan et al.*, 2004; *Pries et al.*, 2013], unfrozen soil layers continuing into the fall [*Mikan et al.*, 2002; *Michaelson*

and Ping, 2003], liquid water in frozen soils [*Sturm et al*., 2005], and cold-adapted plants and microbes [*Bate and Smith*, 1983; *Kappen*, 1993; *Panikov et al*., 2006].

The lack of appropriate technology and the difficulties in making quality trace gas flux measurements in the harsh arctic nonsummer seasons [*Oechel et al*., 1995] have contributed to the current scarcity of data and understanding of CO_2 exchange during such periods [*Sullivan et al*., 2008]. This lack of data coupled with inadequate understanding of the important processes and controls on fluxes in winter has limited our ability to effectively estimate and model current annual CO_2 fluxes. These issues also lead to difficulty predicting with any certainty the annual carbon balance for the Arctic under expected future environmental conditions [*Elberling and Brandt*, 2003].

The assumption that the production of CO_2 during the nonsummer period can be calculated from temperature and Q_{10} relationships (a temperature coefficient describing the increase in respiration as a consequence of a 10°C increase in temperature) has further reduced the impetus for direct CO_2 flux measurements in the winter [*Fang and Moncrieff*, 2001; *Mikan et al*., 2002; *Wang et al*., 2010]. Other factors are important in simulating nonsummer CO_2 efflux including latitude, day of year, snow depth [*Fahnestock et al*., 1998; *Zamolodchikov and Karelin*, 2001; *Elberling*, 2007] as well as the relationship of temperature, ecosystem respiration, and CO_2 efflux. Nonsummer periods can be complicated with respect to the controls on CO_2 exchange. This is particularly true of the transitional seasons when snow is melting or accumulating, and there is a combination of frozen, freezing, and unfrozen soil layers above the permafrost zone [*Kwon et al*., 2006; *Runkle et al*., 2012; *Trucco et al*., 2012]. While some feel that Q_{10} is independent of mean annual temperature and does not differ among biomes [*Mahecha et al*., 2010], respiration is difficult to predict from Q_{10} alone where there is a phase change from frozen to liquid water in under freezing or thawing conditions [*Davidson and Janssens*, 2006].

Simulating net ecosystem CO2 exchange (NEE) may be even more complicated. For example, vascular plants may photosynthesize until below −3°C under the snow [*Bate and Smith*, 1983], lichens and mosses have been shown to photosynthesize down to below −10°C under the snow [*Sveinbjörnsson and Oechel*, 1981; *Walton and Doake*, 1987; *Kappen*, 1993], and microbial respiration has been observed at −40°C [*Zimov et al*., 1996; *Michaelson and Ping*, 2003; *Panikov et al*., 2006]. Increasing respiration rates, and subnivian CO_2 (released during the snowmelt period), may lead to net carbon source events even though radiation and photosynthesis are increasing. This is in apparent contradiction to the general assumption of increased radiation leading to increasing NEE, as is generally observed during the summer season [*Semikhatova*, 1992]. Interacting processes and patterns lead to interesting and complex carbon exchange patterns throughout the year.

The work reported here was undertaken to quantify the annual CO_2 flux and to evaluate the environmental controls on fluxes among key seasonal periods in the Arctic in a moist acidic tussock tundra ecosystem near Atqasuk, Alaska. To accomplish the latter, an objective definition of season based on the radiative energy balance was developed.

2. Materials and Methods

2.1. Site Description and Instrumentation

The study was conducted about 100 km south of Barrow, AK, on Alaska's North Slope near the village of Atqasuk (70°28′10.6″N; 157°24′32.2″W, 24 m elevation), in 2006. The land cover is moist acidic tundra, dominated by a tussock-forming sedge (*Eriophorum vaginatum*) and other vascular species (*Carex Bigelowii*, *Vaccinium Vitis-idaea*, and *Ledum Palustre*), with scattered prostrate shrubs [*Komarkova and Webber*, 1980]. The landscape within the study area is primarily flat, and vegetation height generally does not exceed 0.2 m. Soils are developed on Aeolian sands of Quaternary age [*Everett*, 1980] and consist of approximately 95% sand and 5% clay and silt to a depth of 1 m [*Walker et al*., 1989]. In this area, soils have an organic-rich surface horizon of silt clays to silt loam-textured mineral material, and an underlying perennially frozen organic-rich horizon [*Michaelson and Ping*, 2003]. The depth of soil organic layer ranges to 18 cm below the surface level. Total organic carbon content to a depth of 1 m is 38 kg C m^{-2} [*Tarnocai et al*., 2009]. Owing to the presence of permafrost, soil drainage is poor throughout the summer season. In this area, the active layer depth increases in a nearly linear fashion throughout the summer and does not show a decreased rate of thaw until late summer. The maximum depth of thaw was about 43 cm [*Kwon et al*., 2006]. Snow cover depth varied by time

Table 1. Seasons as Defined by Daily Mean Net Radiation (R_{net}) and Accepted Raw Data Availability by Number of Half Hours and Percentage of Total Half Hours

Season	Daily Mean R_{net} (W m^{-2})	Days of Year by Season	Number of Days per Season	%Raw Data Accepted
Winter	< 0	274–113	205	24
Spring	0–99, postwinter	114–143	30	63
Summer	≥ 100	144–226	83	73
Fall	0–99, prewinter	227–273	47	69

during the year. The snow depth was approximately 0.3 m from January 2006 to 0.5 m in early May 2006 when it decreased until snow melt at the end of May. Snow began to accumulate again in October 2006 reaching 0.3 m in early January 2007 [*Laskowski*, 2010]. The eddy covariance method [*Baldocchi et al*., 1988] was used to assess net ecosystem CO_2 exchange. The CO_2, H_2O, and sensible heat fluxes were measured at a height of 2.5 m above the plant canopy. Carbon dioxide and water vapor measurements were made with a LI-7500 infrared open-path gas analyzer (IRGA; pre-2010 model, LI-COR Biosciences, Lincoln, NE, U.S.). Three-dimensional wind speed, direction, and sonic temperature measurements were made using an ultrasonic anemometer (R3, Gill Instruments, Hampshire, UK). Both instruments operated concurrently at 10 Hz. Other environmental data were recorded every 15 s and averaged over half-hour periods using a CR-23X data logger (Campbell Scientific, Logan, UT, U.S.). Environmental data included temperature and relative humidity (HMP45, Vaisala, Helsinki, Finland), net radiation (Q7 Radiation Energy Balance System (REBS), Seattle, WA, U.S.), photosynthetically active radiation (PAR; LI-190SB, LI-COR Biosciences, Lincoln, NE, U.S.), soil temperature (Type-T thermocouples, Omega, Stamford, CT, U.S.), ground heat flux (HFT-1, REBS, Seattle, WA, U.S.), wind speed (03002 Wind Sentry Set, R. M. Young, Traverse City, MI, U.S.), and precipitation (TE 525, Texas Electronics, Dallas, TX, U.S.).

NEE data were collected continuously throughout the year. Most data loss were related to system malfunctions and quality control procedures based on eddy covariance quality checks [*Lee et al*., 2004]. Nearly 4000 h of raw CO_2 data were accepted in total, representing 44% of all half-hour periods (Table 1). During the spring, summer, and fall seasons, the instruments were visited at least once a week to ensure proper operation, leading to approximately 70% data retention during these seasons. The winter period had lower data retention due to the extreme conditions of Arctic winter. Harsh conditions made it impractical and unsafe to continue the same maintenance schedule as in warmer seasons. Low temperatures often prohibited manipulation of the instrumentation because insulation, wires, and many other system components were highly brittle. Data capture for the winter improved significantly (from below 15% to nearly 40%) in late winter and early spring when instruments could once again be checked at least weekly and cleared of ice, snow, or debris.

2.2. Data Analysis

Average half-hour fluxes of carbon dioxide (NEE) and water vapor fluxes were calculated from raw data using EdiRe software (University of Edinburgh, Edinburgh, Scotland, UK). Two-dimensional wind rotation, despiking routines, and quality control checks of the calculated fluxes followed FluxNet (http://fluxnet.ornl.gov/) guidelines, which coordinates regional and global analysis of observations from micrometeorological tower sites using eddy covariance methods [*Baldocchi et al*., 2001; *Lee et al*., 2004; *Moffat et al*., 2007]. Gaps in the flux data were filled through methodology similar to *Falge et al*., (2001) in combination with the approach described in *Reichstein et al*. [2005], and also with tools from Max Planck Institute for Biogeochemistry (http://www.bgc-jena.mpg.de/~MDIwork/eddyproc/).

Two corrections for air density fluctuations were applied according to *Webb et al*., 1980 and *Burba et al*. [2008]. The former is a well-known term that is used to compensate for the fluctuations of temperature and water vapor affecting measured densities of CO_2, H_2O, and other gases. The latter is a recently developed correction compensating for the additional heat produced by elements surrounding the open sampling path of the pre-2010 model of LI-7500 gas analyzer. The open sampling cell of the analyzer is bound by source and detector windows and by support spars. These components of the instrument may have temperatures different from those of ambient air due to internal electronics, and radiative and convective heating and cooling of the surfaces. Such phenomenon can lead to additional temperature variation in the sampling path, which is especially important at low ambient temperatures. This has been shown to cause a departure

between the air temperatures measured at 10 Hz by the sonic anemometer and the actual air temperatures within the optical path of the open-path IRGA [*Grelle and Burba*, 2007]. The size of the heating correction was quite small ranging from zero to about 0.6 μmol of CO_2 m^{-2} s^{-1} for most cases [*Burba et al*., 2008]. This is 10–50 times smaller than standard eddy covariance flux corrections, such as the open-path Webb-Pearman-Leuning (WPL) corrections or closed-path frequency response corrections, and similar in magnitude to open-path frequency response corrections. However, if uncorrected, the small bias can lead to apparent sink observed instead of zero fluxes or very low positive fluxes and can lead to an overestimation of net ecosystem uptake when integrated over longer periods in cold environments [*Grelle and Burba*, 2007; *Clement et al*., 2009; *Burba et al*., 2008; *Clement et al*., 2009; *Jarvi et al*., 2009; *Massman and Frank*, 2009; *Reverter et al*., 2011].

The surface-heating correction was applied to all CO_2 flux data, after it was adjusted to reflect specific application and site conditions different from those in which the correction was tested [*Grelle and Burba*, 2007; *Burba et al*., 2008; *Jarvi et al*., 2009], notably an inclined IRGA, lower ambient temperatures, strong winds, possible snow and ice deposits on the parts of the instrument, etc. The correction was calibrated by identifying periods when change in CO_2 efflux with temperature can be assumed to be nearly negligible, calculating the correction factors accordingly and applying them to the full set of measurements. The conditions for negligible change-in-flux periods were the following: (i) 3 months after the soil was frozen continuously, (ii) soil remains frozen, (iii) air temperatures remain below −35° C. Minimal rates of carbon exchange are expected under these conditions [*Zimov et al*., 1993; *Elberling*, 2007]. The derivation of "daytime" and "nighttime" temperature relationships described in *Burba et al*. [2008] were applied here to high- and low-radiation conditions (i.e., >50 W m^{-2} and ≤ 50 W m^{-2}, respectively). Missing data for input parameters were filled with data available from nearest weather stations or by interpolation. In particular, wind speed data were filled using Department of Energy's Atmospheric Radiation Measurement site (http://www.arm.gov/) located about 250 km to the east of the study site, but highly correlated with the site ($R^2 = 0.93\%$), while CO_2 and H_2O densities were filled by interpolation.

It is important to note that this method of applying the correction results is a conservative estimate of actual CO_2 efflux. It is likely that diffusion through the snowpack may result in a small net source of CO_2 [*Panikov et al*., 2006] which can change in intensity with temperature even under the coldest conditions. So while we assumed no CO_2 efflux below negative 35° C, there was undoubtedly some low levels of CO_2 efflux [*Oechel et al*., 1993]. Therefore, the actual CO_2 efflux values are most probably larger than those reported here. The full adjustment procedure is described in detail in Appendix A.

In this study, the year was divided into seasons as follows. Spring season begins when daily average net radiation (R_{net}) > 0 W m^{-2} for three or more consecutive days. Summer begins when three consecutive days are measured at $R_{net} > 100$ W m^{-2} and ends at the last period of three consecutive days of $R_{net} > 100$ W m^{-2}. Fall is the period after summer and lasts until there are three consecutive days when R_{net} is below 0 W m^{-2}. The period between fall and spring, as defined above, is winter. While multiple definitions of seasons exist in literature [*Griffis et al*., 2000; *Laurila et al*., 2001; *Arneth et al*., 2002], here we chose a definition based on quantifiable physical characteristics based on net radiation. It was found that this approach worked well, as it captured the changing conditions of light and energy, generally responsible for ecosystem dynamics thought the year.

To determine the specific environmental controls on carbon exchange within each season, NEE fluxes were analyzed as a function of the key controlling variables (air and soil temperature, net radiation, photosynthetic photon flux density, and wind speed) using stepwise multiple linear regression implemented in the MATLAB software; version 2010b (The Math Works, Natick, MA, U.S.). A linear model was adopted after tests made with more complex functional relations, such as saturating light response, revealed no significant improvement in explanatory capability. First, variables used as regressors and fluxes were averaged to produce hourly resolution diurnal courses for each season, with associated uncertainty computed at the 95% confidence interval. Then, multiple regression was applied in stepwise mode starting with a single regressor. Additional regressors were included in a linear model only when the explanatory power of the model and the statistical significance were significantly improved. Assigned tolerances on model significance were used either to exclude ($p > 0.05$) or include ($p < 0.025$) regressors. All statistical models were defined significant at $p < 0.05$. Uncertainties associated to both the regressors and the fluxes were propagated to the model coefficients (Table 4), giving overall uncertainty estimates.

Table 2. Mean (±Standard Deviation) Daily Environmental Conditions by Season and Annually[a]

Season	T_{air} (°C)		T_{soil} (°C)		R_{net} (W m^{-2})		WS (m s^{-1})		H (W m^{-2})		LE (W m^{-2})	
Winter	−20.57	(10.8)	−11.81	(6.8)	−10.71	(14.1)	4.18	(2.6)	−7.18	(10.0)	0.57	(2.8)
Spring	−7.78	(6.4)	−8.6	(5.3)	13.45	(36.6)	4.00	(1.6)	7.32	(16.9)	3.93	(5.7)
Summer	6.47	(5.2)	6.6	(4.3)	118.59	(130.0)	3.86	(1.7)	36.51	(47.6)	33.35	(33.7)
Fall	3.00	(3.8)	3.56	(2.5)	42.94	(73.1)	3.13	(1.5)	11.81	(29.3)	13.92	(17.8)
Annual	−10.33	(14.9)	−5.42	(10.0)	27.59	(86.5)	3.96	(2.2)	6.39	(31.9)	10.02	(22.0)

[a]T_{air} is average air temperature at 2 m; T_{soil} is average soil temperature at 5 cm depth; R_{net} is net radiation; WS is wind speed; H is sensible heat flux; and LE is latent heat flux.

The Q_{10} of all dark periods was calculated based on exponential regression using CurveExpert Professional 2.0 software. The resultant regression provided the temperature sensitivity of ecosystem respiration for each of the periods analyzed. Short-term (over a month) and longer-term (over the entire year when dark periods existed) periods were analyzed.

3. Results

Average annual air temperature at the study site was −10.3°C (Table 2); minimum daily average temperature was −39.7°C on 1 February, and maximum daily average temperature was 17.0°C on 25 July. Soil

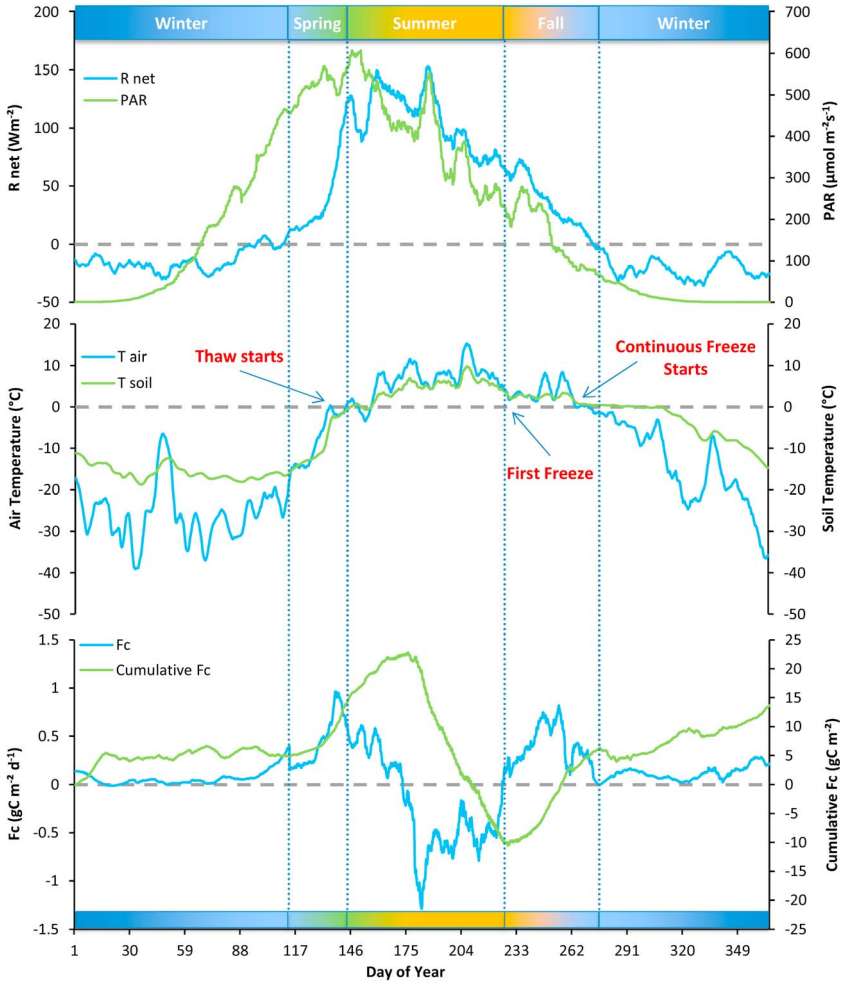

Figure 1. Average daily net radiation, PAR, air temperature, and soil temperature (at −5 cm), daily CO_2 flux, and cumulative CO_2 flux over the year.

Table 3. Seasonal and Annual Total and Daily Rates of Net CO_2 Exchange (Positive Values Connote Release to the Atmosphere)

Season	Seasonal or Annual Carbon Exchange (g C m^{-2} $season^{-1}$)	Average Daily Carbon Exchange (g C m^{-2} d^{-1})
Winter	12.9 ± 0.73	0.06
Spring	9.1 ± 0.32	0.30
Summer	−24.3 ± 1.23	−0.29
Fall	15.9 ± 0.70	0.34
Annual	13.6 ± 1.62	0.04

temperatures at 5 cm depth were more moderate, with an annual average of −5.4°C, minimum of −21.1°C, and maximum of 15.4°C. Annual rainfall totaled 83.7 mm, falling predominantly during July–September. Daily carbon exchange rates for the entire study year are shown in Figure 1. Daily CO_2 exchange rates were varied through the year, ranging from −1.29 g C m^{-2} d^{-1} during peak growing season (2 July) to +0.96 g C m^{-2} d^{-1} (21 May) during the rapid snowmelt, with negative numbers indicating net ecosystem CO_2 uptake. The net annual exchange for this site was a net source of +13.6 ± 1.62 g C m^{-2} yr^{-1} (Table 3) to the atmosphere.

Winter, as defined here, was the longest season in 2006 and lasted 205 days, from 1 October to 23 April (Note, this period is discontinuous as a calendar year was chosen for analysis (Table 1).). Soil temperatures throughout winter were nearly 9°C warmer than air temperature (Table 2). There was only a very slight diurnal pattern of carbon exchange and little net daily activity (Figure 2) due to low solar radiation and cold temperatures. Daily CO_2 flux in winter exhibited a maximum release of 0.39 g C m^{-2} d^{-1} and an average daily exchange of 0.06 g C m^{-2} d^{-1}.

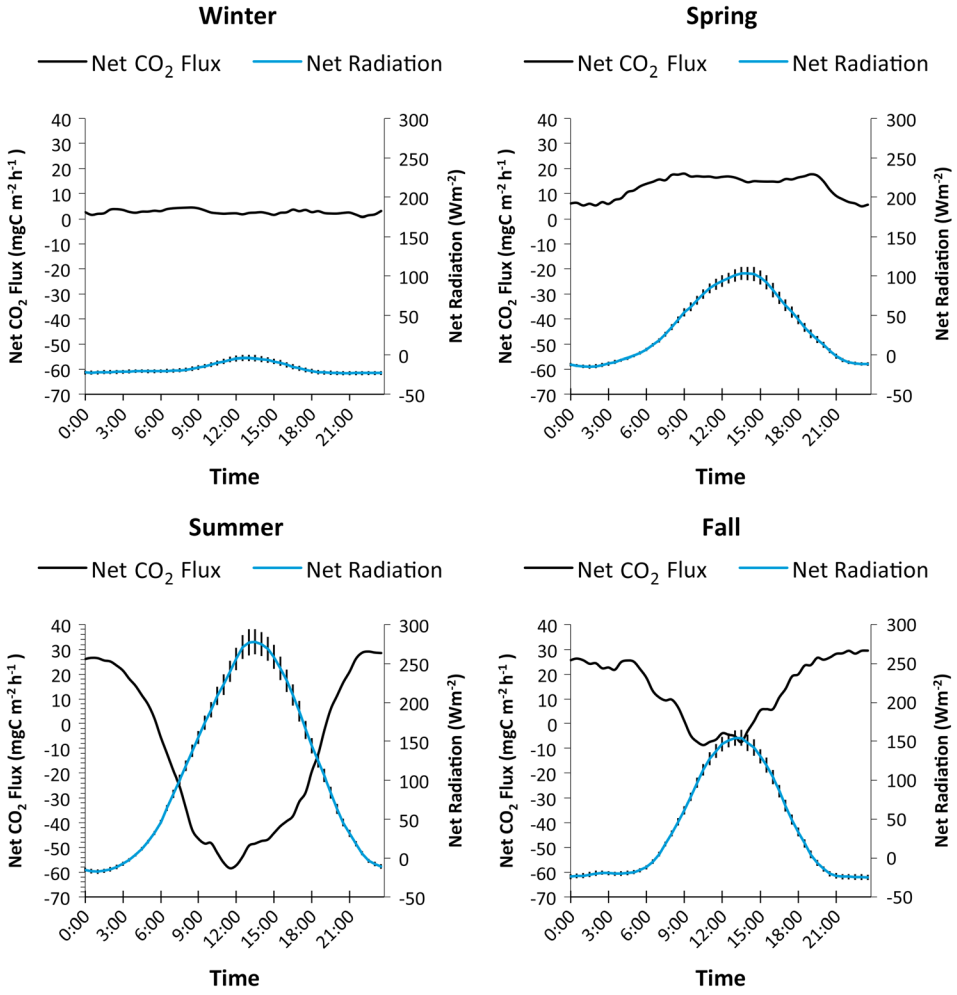

Figure 2. Diurnal pattern of carbon exchange (milligram of Carbon per square meter per hour) and net radiation (Watt per square meter) by season. The error bars are at 95% confidence intervals.

Table 4. Results of Multiple Stepwise Regression Between Seasonal Hourly Averaged CO_2 Fluxes and Environmental Variables[a]

	Hourly	
	Control/s (Normalized Coefficient)	R^2
Winter	R_{net} (+0.50 ± 0.39)	0.24
Spring	R_{net} (+8.86 ± 1.47)	0.90
Summer	R_{net} (−43.59 ± 6.28), T_{soil} (+18.36 ± 6.31)	0.96
Fall	R_{net} (−10.50 ± 6.87), T_{soil} (+4.81 ± 1.77)	0.89

[a]Only significant ($p < 0.05$) variables are reported, with normalized regression coefficient/s uncertainties and associated coefficient of determination (R^2).

Although the daily carbon exchange rate in winter was the lowest of any season, the winter season made a substantial cumulative contribution to the annual carbon budget due to its long duration. The total annual winter efflux was 12.9 ± 0.73 g C m^{-2} (Table 3).

Spring was the shortest season (30 days for 2006, Table 1) with a modest diurnal pattern (Figure 2), yet it was important in terms of carbon exchange due to significant increase in daylight and net radiation. Due to the short duration of the spring period, the cumulative carbon exchange in spring was the smallest of any season despite the fact that the average daily exchange rate was higher than both winter and summer. The greatest daily carbon release was measured at the end of spring (0.96 g C m^{-2} d^{-1}), when snowmelt occurred. There was no carbon uptake detected during this period, and the cumulative carbon exchange was 9.1 ± 0.32 g C m^{-2} (Table 3), which is equivalent to an average daily release of 0.3 g C m^{-2}.

Summer was the season that coincided most closely with the "growing season," and lasted from 24 May to 14 August in 2006 (83 days; Table 1). Diurnal patterns of carbon exchange during summer showed strong midday uptake of up to 58 mg C m^{-2} h^{-1} and nighttime release of half that rate, 29 mg C m^{-2} h^{-1} (Figure 2). Peak carbon exchange occurred at noon (1200 AST). The greatest daily uptake was seen during this season in midsummer (−1.29 g C m^{-2} d^{-1}, on 2 July). Summer showed a net uptake of carbon over the season of 24.3 ± 1.23 g C m^{-2} (Table 3).

Fall contributed a net efflux to the atmosphere of 15.9 ± 0.70 g C m^{-2} (Table 3), and although some carbon uptake occurred, the fall had the greatest average daily carbon release rate (0.34 g C m^{-2} d^{-1}). Average air temperature fell by more than 3° from summer, averaging 3.0°C, while nearly 15 mm rainfall occurred over the 47 day period. Soils continued to thaw, but at a slower rate than during summer. A distinct diurnal pattern in the CO_2 exchange was discernible during fall, but of smaller magnitude than in summer (Figure 2).

3.1. Statistical Analysis

Multiple regression analysis results are reported in Table 4. In winter, a positive control of net radiation (R_{net}) on fluxes was observed on an hourly timescale, while no significant relationship between fluxes and temperature was observed. In spring, R_{net} was significantly related to average hourly NEE, with very high explanatory power ($R^2 = 0.90$) and positive sign (i.e., higher radiation drives more positive fluxes). No significant improvement was achieved by combining more variables in stepwise mode regression. This may be due, in part, to the high correlation between additional regressors and R_{net}. In summer, the linear model selected the combination of R_{net} and T_{soil} as providing the highest, significant, explanatory power ($R^2 = 0.96$). Similarly in autumn, R_{net} and T_{soil} were the main controls on fluxes, with negative sign between R_{net} and fluxes, and positive between T_{soil} and fluxes (Table 4). Uncertainties in Table 4 have been computed by propagating 95% confidence intervals associated to average environmental variables and CO_2 fluxes into linear regression, to take into account both original variability and the regression uncertainty.

Overall, net radiation was a significant predictor of fluxes in all seasons, while soil temperature added a statistically significant improvement of explanatory power in summer and fall.

Table 5. Cumulative Rates of Carbon Exchange as Data Were Originally Collected, With the WPL Correction and the WPL and Burba Correction Applied

Season	Uncorrected Original (g C m^{-2} $season^{-1}$)	Corrected WPL (g C m^{-2} $season^{-1}$)	Corrected WPL + Burba (g C m^{-2} $season^{-1}$)
Winter	−71.3	−34.1	12.9
Spring	−79.0	1.2	9.1
Summer	−181.3	−47.3	−24.3
Fall	−22.0	6.5	15.9
Total	−354.6	−73.6	13.6

3.2. Impact of Correction Factors

Both the WPL and Burba corrections were nonnegligible throughout the year, although the WPL correction had a much greater absolute impact on flux than the Burba correction (Table 5). Because the raw CO_2 exchange values were often very small, the percent contribution by either factor on a daily or hourly basis was highly variable. Over an entire year, the noncorrected carbon exchange was $-354\,g\,C\,m^{-2}\,yr^{-1}$, and the WPL-corrected value was $-73.6\,g\,C\,m^{-2}\,yr^{-1}$. Applying the WPL correction adjusted for surface heating yielded a net efflux of $+13.6\,g\,C\,m^{-2}\,yr^{-1}$. In the spring and fall, applying the WPL correction changed the cumulative carbon exchange from a sink to a source, and the surface heating correction augmented the source strength. Summer was the only season in which the raw, WPL-corrected, and WPL + Burba corrected data have the same sign, in each case showing uptake (Table 5). The net effect of the WPL correction on the original data was on average 7 times that of the surface heating, but both corrections were important for accurate results under Arctic conditions.

3.3. Q_{10} Analysis

The Q_{10} analysis was calculated based on an exponential regression model for respiration for all dark periods. The calculation of respiration was done during dark periods when PAR was less than $10\,\mu E\,m^{-2}\,s^{-1}$. Q_{10} was calculated against temperature for each month with a dark period, and also during different months of the year for every 10°C increase in temperature. The four summer months of June, July, August, and September are not included in this analysis due to the lack of a dark period (Figure 4). These monthly and near annual Q_{10} values can be helpful in gap filling Arctic respiration data and in Earth simulation models when dealing with Arctic ecosystems. Since the longest period considered was less than a year, these results do not include the longer-term effects of acclimation and adaptation and therefore will likely overestimate the long-term effects of global warming on ecosystem respiration. In general, if other factors are not limiting, increasing temperature will lead to an increase in ecosystem respiration. This increase is only appropriate until the temperature reaches a threshold that would result in damage to vegetation. Global earth simulation models often use Q_{10} values of 2 or below to simulate regional and global carbon dynamics. However, these analyses do not account for both regional and seasonal effects and the apparent effect of phase change (freezing and thawing of the soil layers) on Q_{10}. In addition, the process of respiration acclimating to temperature affects the respiration rate, and therefore the apparent or effective Q_{10}. To clarify Q_{10} calculated over the span of months will be quite different from Q_{10} calculated over the span of hours or days; this is due the effects of acclimation [see, e.g., *Oechel et al*., 1981].

4. Discussion

The annual carbon exchange for the study period was a net efflux of $+13.6 \pm 1.62\,g\,C\,m^{-2}$ (Table 3). Nearly half of the raw data were retained in the final analysis. This is a higher percentage than other continuous eddy covariance systems, including those in nonextreme environments [*Wilson et al*., 2002]. Because of the thermal mass involved, because the soil is insulated by a layer of snow in the winter, and because gaps in data were sporadic, even 15% data coverage in winter could be used to estimate winter fluxes. The winter season was the longest period and had the lowest fluxes and the greatest data loss. This season was generally characterized by below-freezing air temperatures and a snow layer that insulated the ground. At the beginning of winter, the ground was generally freezing bidirectionally (i.e., from the surface downward and from the bottom of the active layer upwards), or fully frozen. In this study, winter showed the lowest daily carbon exchange rates of any season (Figure 2), but the ecosystem still lost a very substantial amount of carbon due to the length of the winter period (Table 1). Daily average temperature variability was very low ($1\sigma \sim 1$°C for T_{air} and $1\sigma \sim 0.1$°C for T_{soil}), resulting in a significant relationship between the ecosystem's respiratory fluxes and air temperature, while a moderate positive control of R_{net} on fluxes was observed (Figure 2). The relatively stable fluxes, characterized by low temporal variability, allowed for extrapolation of high-quality data to the entire winter period. This made it possible to obtain a reliable seasonal estimate, despite the data loss that did occur due to the difficult winter conditions.

The spring period is distinct in the Arctic due to rapidly increasing radiation and rising daily temperatures. As snowmelt begins, accumulated subnivian carbon dioxide may be released. In addition, exposed patches of ground with a lower albedo begin to warm as they absorb radiation, further enhancing respiration rates and CO_2 release to the atmosphere. This situation creates physical and biological conditions that generally favor

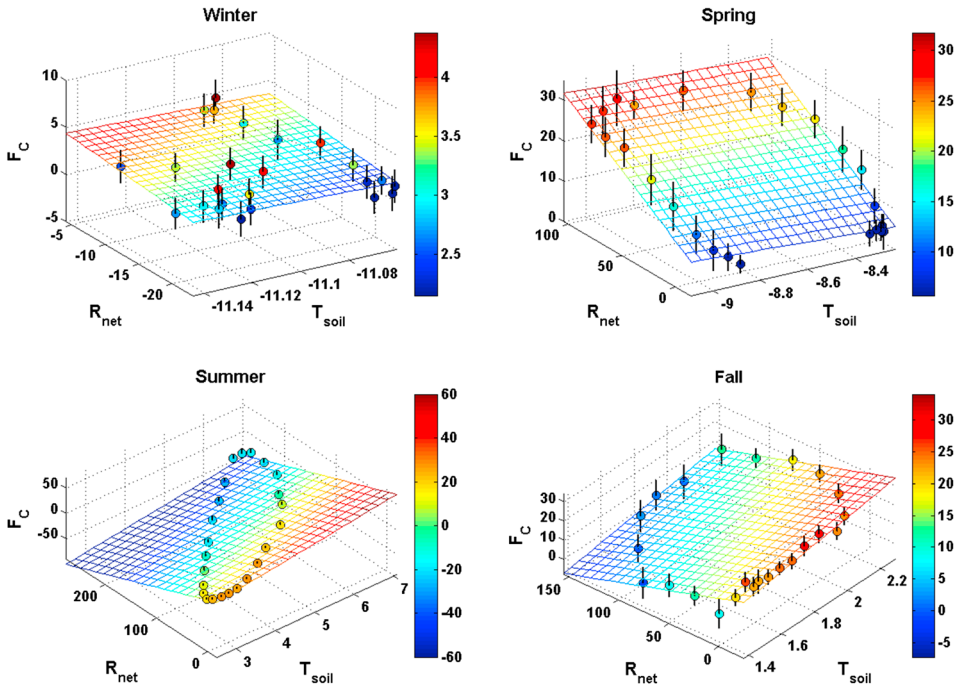

Figure 3. Seasonal hourly averaged CO_2 fluxes (milligram of Carbon per square meter per hour) and associated 95% confidence intervals plotted against soil temperature (degrees Celsius) and net radiation (Watt per square meter). The two-dimensional fitting response surface is reported and colored for CO_2 flux magnitudes (right color bars in milligram of Carbon per square meter per hour).

CO_2 release from the soil, while photosynthetic CO_2 uptake may also occur. Because of its short duration, spring contributed the least to the annual carbon budget (9.1 g C m^{-2}) of any season, yet showed high daily exchange rates (0.3 g C m^{-2}) (Table 3).

During spring, incoming radiation reaches levels adequate for photosynthesis, even under the snow [*Weller and Holmgren*, 1974; *Starr and Oberbauer*, 2003]. The combination of increasing light, along with increases in soil temperatures can result in early photosynthesis and increased respiration [*Oechel*, 1976; *Kutzbach et al*., 2007]. This depends on other conditions such as maximum thaw depth and growing degree days at the time in this year. Physical factors also play an important role in this season, as large and rapid carbon efflux can occur due to release of carbon accumulated below the snow [*Friborg et al*., 1997]. Our data show that respiration exceeded photosynthesis in the spring resulting in a positive average flux to the atmosphere, with a slight diurnal pattern of NEE. Several environmental variables were highly and positively correlated with each other, making distinguished of controlling factors challenging. This include air temperature and soil temperature ($r^2 = 0.7$), net radiation and visible radiation (photosynthetic photon flux density) ($r^2 = 0.51$), and air temperature and net radiation ($r^2 = 0.2$). Net radiation alone explained the greatest variation in NEE in the spring through a positive control (Figure 3 and Table 4).

The summer season was the only season to show net carbon uptake. This season encompassed the greening of the tundra and showed strong diurnal CO_2 flux patterns (Figure 2). This indicates a short-term (i.e., diurnal) response to temperature and light conditions, which has been explored elsewhere in detail [e.g., *Kwon et al*., 2006; *Zona et al*., 2009; *Laskowski*, 2010]. Summer was unique in many of the functional relationships when compared with the rest of the year. Multiple linear regression results indicate a strong, negative relationship between net radiation and NEE (a positive flux is a release of CO_2 to the atmosphere), likely related to higher available radiative energy resulting in higher photosynthesis rates. Soil temperature showed a positive relationship with NEE, likely related to the positive control of temperature on respiration (Figure 3 and Table 4) that was also observed by *Mahecha et al*. [2010]. All else remaining constant, earlier initiation of summer may result in longer season leading to a greater photosynthetic uptake and a negative feedback on global warming. However, any changes in the hydrology, soil aeration, and soil temperature following a longer snow-free period, could increase soil respiration and reduce the summer sink, or even result in a

Table 6. Cumulative Rates of Carbon Exchange for Various Growing Season Periods Based on Different Definitions of Growing Season

Summer Season Period	Cumulative Carbon Exchange (g C m^{-2} $season^{-1}$)
1 May to 1 September	−1.6
17 May (melt date) to 31 August	−7.3
1 June to 31 August	−13.8
24 May to 14 August (this study)	−24.3
14 June to 31 July	−17.8
1 July to 1 August	−19.3

summer source of CO_2 to the atmosphere [see, e.g., *Oechel et al*., 1993; *Lund et al*., 2012]. This supports the possibility that future increases in temperature may weaken the CO_2 sink strength for this ecosystem during summer. Summer CO_2 loss to the atmosphere may even be possible, depending on changes in vegetation structure and functioning as a response to a changing climate [*Lund et al*., 2012].

The fall season made a significant contribution to the annual carbon budget, accounting for a loss to the atmosphere of +15.9 g C m^{-2}. Day length decreased during this period, and air and soil temperatures generally declined. Weakened but distinctive diurnal patterns were still observed during this season (Figure 2). During the fall, soil temperatures were still adequate for substantial microbial respiration. When the senescence of vascular plants advanced, respiration became the dominant process affecting carbon exchange (*Semikhatova*, 1992). In addition, as soils freeze, CO_2 may be forced out of the soil solution as the soils freeze [*Coyne and Kelley*, 1971], ultimately making its way to the atmosphere. Of the variables tested, net radiation and soil temperature were the dominant environmental controls on carbon flux in this study (Figure 3 and Table 4). They reflected both the "residual" photosynthetic capacity observed at high midday net radiation in the diurnal cycles (Figure 2), and the overall increase in respiration as the season proceeds and radiation decreases (Figure 1).

Dividing the year into functional seasons allows evaluating the impacts of relative changes in the duration of each of the seasons, and then evaluating how changing conditions within the seasons may affect annual CO_2 flux. A season can be defined in numerous ways, including based on calendar dates [*Griffis et al*., 2000; *Arneth et al*., 2002] and by visual observations [*Laurila et al*., 2001]. Different definitions affect the calculated dates and length of each of the seasons, and as a result, the calculated seasonal uptake. Accordingly, we used five common definitions to estimate the growing season allowing us to determine how the definition of summer affected the calculated summer CO_2 flux (Table 6).

The method of seasonality based on surface energy availability is proposed here because it has a biophysical basis, is easily quantified, and is easily applied. In addition, this method is amenable to interpolation of carbon flux where climate variables are known but where eddy covariance measurements may not be feasible. Also, a net energy flux calculation captures effects of incoming radiation (including light) and the presence of snow cover and is important determinant to plant activity. Literature reports define growing season starting anywhere from day of year (DOY) 164 (13 June) to DOY 238 (26 August) in tundra in 1997 [*Griffis et al*., 2000] and ending anywhere from DOY 226 (13 August) in 2000 to DOY (20 August) in 2003 [*Groendahl et al*., 2007] (Table 6). The scheme, based on seasonal values of net radiation, inherently captures changes in the snow-free period, especially earlier snowmelt. This variable in particular has been observed to be approximately 2 weeks earlier over two recent decades [*Myneni et al*., 1997; *Michaelson and Ping*, 2003; *Groendahl et al*., 2007] because of the decrease in reflected energy with the disappearance of snow cover.

The importance of net radiation as an important driver is supported by regression analysis, revealing that net radiation is the most significant correlate with hourly fluxes in all seasons (Table 4). Available energy, which is associated with soil temperature affects both CO_2 uptake through photosynthesis and loss through respiration. Therefore, the sign for net radiation or temperature can either be positive or negative throughout the year (Figure 3). Separating NEE into the contributing process of photosynthesis (gross primary product) and ecosystem respiration (R_{eco}) still remains a challenge. Classical flux partitioning approaches, based on the nighttime flux-temperature dependence and its extrapolation to daytime fluxes, become extremely uncertain in arctic conditions because of the long period with no nighttime dark period, and because they assume dependencies between respiration and environmental controls (especially temperature) that may vary over the day and the season. However, extrapolating the ecosystem light response curve back to zero light, for various temperature classes, seems the best way to determine summer Reco as a function of temperature.

The annual carbon budget presented here is based on measurements made throughout the year including January and February. To our knowledge, it is the most comprehensive annual data set available for the Arctic

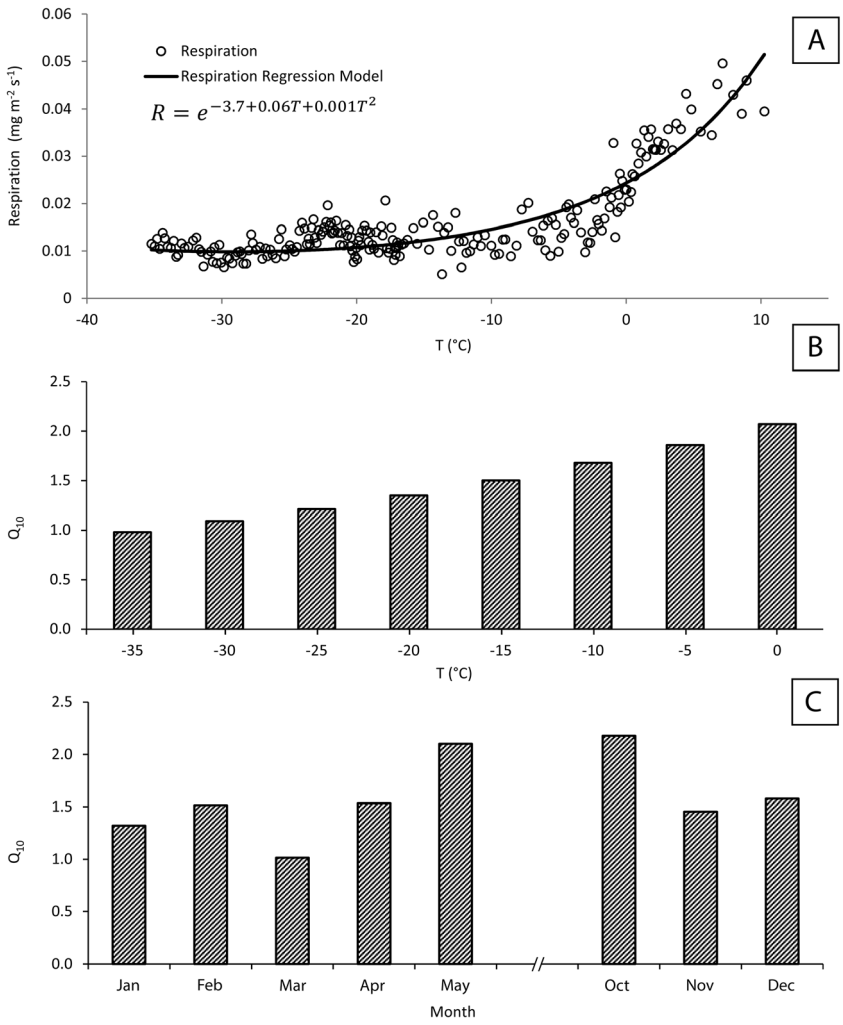

Figure 4. (a) Respiration rate for all data and seasons for fluxes (milligram per square meter per second) with dark conditions (PAR $< 10\ \mu E\ m^{-2}\ s^{-1}$) versus air temperature (degrees Celsius) and the corresponding exponential regression; (b) Q_{10} relationship for every 10°C interval for all dark data; (c) Q_{10} for all months of the year with a dark period of PAR $< 10\ \mu E\ m^{-2}\ s^{-1}$. The four summer months of the year are excluded from this analysis since there was no dark period.

to date. This year-round set of observations demonstrates that (i) the importance of nonsummer fluxes in the annual carbon budget is overwhelming, and (ii) the functional relationships of environmental variables and carbon exchange vary significantly by season.

Other studies have measured carbon exchange at various points throughout the year, but generally extrapolated a relatively few cold season measurements to calculate the annual budgets [*Welker et al.*, 2000; *Corradi et al.*, 2005; *Elberling*, 2007]. As demonstrated above, there is important temporal variation in nonsummer fluxes that could easily bias the results under sparse sampling. In addition, the combination of factors affecting cold season CO_2 flux are complicated, nonlinear, and vary by season. An improved understanding of the processes that form the major controls on CO_2 exchange during each of the seasons, along with continuous, year-round sampling will lead to a better understanding the current Arctic carbon budget and will help provide the tools to better predicting future changes in this critical landscape.

Predicting current and future NEE related to temperature requires estimating ecosystem respiration as a function of temperature and other changing environmental conditions. Q_{10} is often used to calculate the effect of temperature on respiration rates. However, Q_{10} can be known to change by temperature, season, and conditions (e.g., the thaw state of the soil). The Q_{10} values presented here were determined over short-term periods (daily time steps over a month) and over the entire year when there was a dark period (some of

the spring and much of the summer was therefore excluded from the analysis) (Figure 4). The availability of Q_{10} values obtained throughout the year (when there is a dark period of < 10 μE m^{-2} yr^{-1}) will be helpful in improving the estimated annual NEE and simulations of NEE under future conditions. Also, the period of soil freeze thaw may have an effect on Q_{10}, or at least on respiration rates [*Zona et al*., 2011]. The highest Q_{10} rates are seen during the period of thawing or freezing soils in spring and fall (Figure 4c).

Appendix A: Adjustment of the Open-Path Surface Heating Correction for the Inclined Analyzer

Due to the cylinder-like geometry, the bottom portion of the severely inclined instrument in Alaska is exposed to winds, sun, sky, and other elements quite differently in comparison with the vertical instrument tested in Nebraska and described in detail in *Burba et al*. [2008]. This difference may be particularly important during polar night, when the inclined cylinder is exposed to a radiatively black sky to a larger extend than the vertical cylinder. At the same time, the top portion of the instrument is geometrically close to a ball shape and, on average, is not affected by inclination as much as the cylinder.

The study employed extremely remote low-power eddy covariance station, with minimal number of measurements required for confident flux calculations and could not provide essential parameters required for constructing the energy budget of the instrument surface based on fundamental physical principles (e.g., measured instrument surface temperatures, incoming and outgoing long-wave radiation, and amounts of snow and ice on the instrument surfaces). In the absence of such key parameters, for this adjustment we assumed that the temperature exchange for the bottom cylinder may be different in Alaska versus Nebraska, as well as respective temperature regressions for day and night, and that this difference contributes most to the differences between the heating of the vertical sensor in Nebraska and the inclined sensor in Alaska.

The inclined bottom cylinder in Alaska was assumed to be more exposed to the elements than the vertical cylinder in Nebraska, and its temperature (T_{botAK}) was assumed to be a combination of the bottom cylinder temperature in Nebraska (T_{botNE}) and the top ball temperature in Nebraska (T_{topNE}). The latter was assumed to be similarly exposed to elements in Nebraska and Alaska but is always more exposed to elements than the bottom cylinder.

$$T_{botAK} = xT_{botNE} + (1 - x)T_{topNE}, \quad \text{(A1)}$$

where x is a weighting factor.

The x in equation (A1) was parameterized during only very cold periods with an air temperature below −35°C in January–March 2006, 3 months after the soil was frozen and CO2 could have been pushed out. It is

Table A1. The Bounding Conditions for the Adjustment of the Inclined Sensor in Alaska[a]

	x for T_{botAK} (%)		Slope of F_c versus Air T, at $T_a < -35$°C, (×1000; the Closer to Zero the Better)	Number of Negative Daily Corrections at Air $T < 0$°C (the Smaller the Better)
	T_{botNE}	T_{topNE}		
Adjustment for inclined sensor in Alaska	0	100	0.900	161
	50	50	0.080	48
	55	45	−0.002	15
	60	40	−0.085	6
	61	39	−0.102	3
	62	38	−0.119	3
	63	*37*	*−0.135*	*1*
	64	36	−0.152	1
	65	35	−0.169	1
	70	30	−0.250	0
	80	20	−0.420	0
	90	10	−0.580	0
	100	**0**	**−0.750**	**0**

[a]It is highly unlikely that CO_2 flux (F_c) will change significantly with air temperature at ambient conditions below −35°C in January–March, after soil was frozen for over 3 months (e.g., October–December). It is also implausible to expect the large number of occurrences of negative heating correction (e.g., meaning the instrument is colder then ambient) at ambient temperatures below 0°C, because instrument electronics is kept at about +30°C. Optimal weighting for x was chosen at minimal slope of F_c versus T at 1 occurrence of negative correction, which magnitude was not statistically different from zero. Italicized values indicate optimal values while those in bold are values for vertical sensor in Nebraska.

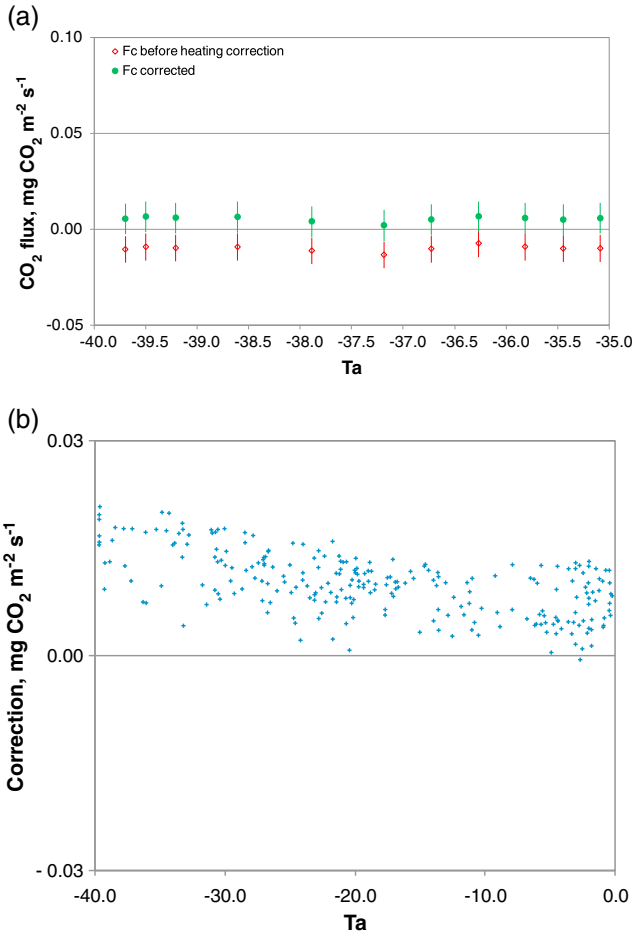

Figure A1. The bounding conditions described in Table A1. (a) With 63% to 37% weighting, the corrected daily CO_2 fluxes at temperatures below −35°C had minimal slope with air temperature and were not significantly different from zero. (b) At the same time, there was only one occurrence of the negative daily correction at temperatures below −0°C, which magnitude was not statistically different from zero as well. Increasing the weighing factor created steeper CO2 flux-to-air temperature slope, which is highly unlikely physiologically, and is not supported by the data from literature. Decreasing the weighting factor resulted in the large number of occurrences of negative daily corrections which is implausible from the fundamental thermal exchange between the instruments controlled at +30°C and subzero air temperature.

reasonable to assume during such periods that the CO2 flux should not change with temperature varying from −35 to −40°C. The closeness of the CO_2 flux-to-air temperature slope to zero became first criterion for the best *x*, and no assumptions were made on the actual magnitude of the CO2 flux.

Then, the corrections were computed using Method 4 (submethod: linear regression with air temperature) [*Burba et al*., 2008] for multiple weighing factors *x*, resulting in different CO_2 flux-to-air temperature slopes. The magnitude of the corrections were then examined over a different, much broader cold period when air temperature was below 0°C. During such periods, the daily correction should not become negative, as this would suggest that the instrument is cooler than ambient air. The latter is implausible because old model of the instrument was controlled at about +30 C, and should on average be warmer than the subzero air temperatures. The minimal number of days with negative correction became the second criterion for the best *x*.

By using both criteria (the near-zero slope of the CO_2 flux-to-air temperature curve below < -35 C, and the minimal number of negative corrections below 0 C), the adjustment was bound based on a basic physiology of the ecosystem and physics of the thermal exchange of the instrument, and without any assumption on what CO_2 flux magnitudes should actually be. All parameterizations were done based on 24 h of data to eliminate methodological and instrumental noises during these cold periods with diminutive fluxes.

Table A1 illustrates this procedure. The optimal weighting came out at 63% to 37%, such that $T_{botAK} = 0.63\ T_{botNE} + 0.37\ T_{topNE}$. This way the CO_2 flux did not significantly change with *T* below −35°C, and nearly all heating correction occurrences were positive or near zero. Increasing the weighing factor above 63% created steeper CO_2 flux-to-air temperature slope, which is highly unlikely physiologically and is not supported by the data from literature. The original correction developed for vertically oriented sensor in Nebraska ($x = 100$) would have led to a slope 5.5 times steeper that observed for optimal *x* in Alaska. Decreasing the weighting factor below 63% resulted in the large number of occurrences of negative daily corrections which were implausible from the fundamental thermal exchange between the instruments controlled at +30°C and subzero air temperatures.

The resulted fluxes during the periods with air temperatures below −35 C are shown in Figure A1a. The fluxes before the correction were small, but significantly negative, suggesting small CO2 uptake. After the

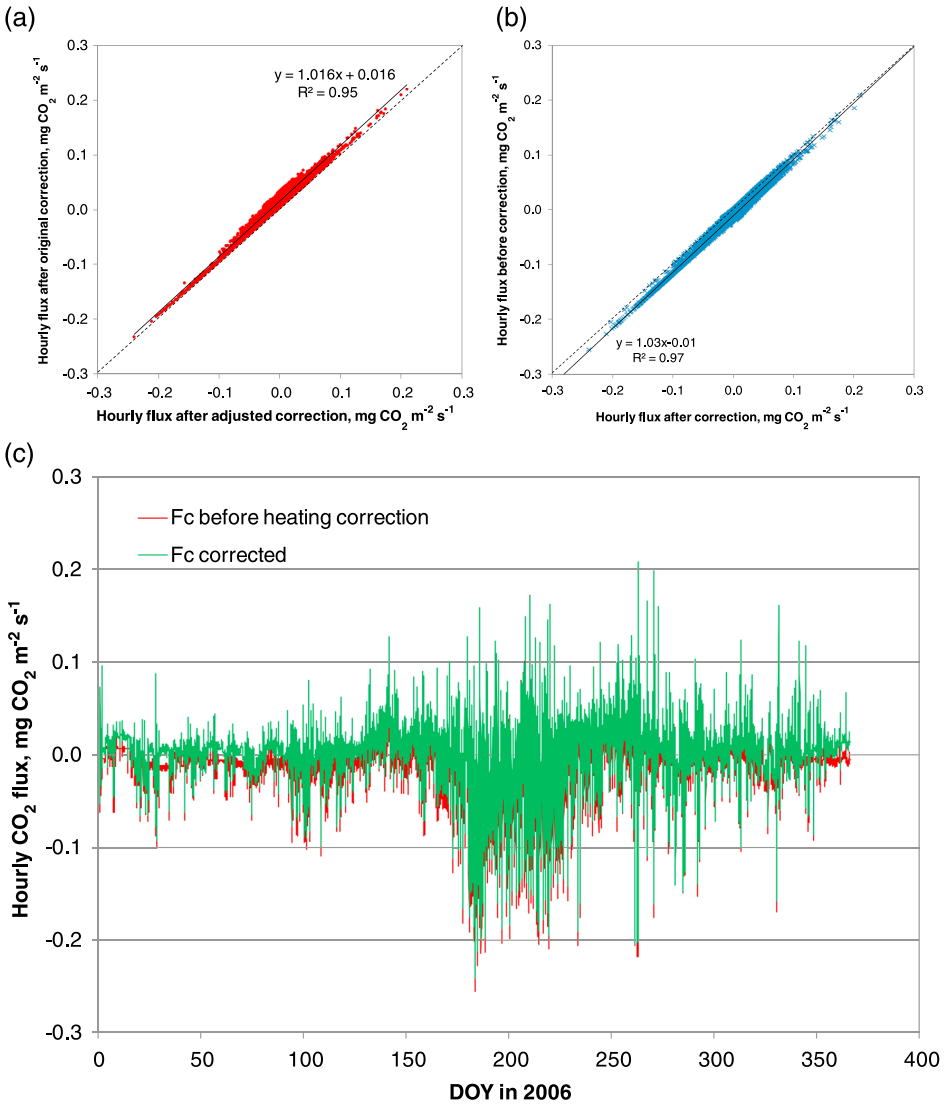

Figure A2. Hourly fluxes for the entire year. (a) The fluxes after original surface heating correction [*Burba et al.*, 2008] plotted versus the fluxes corrected with an adjustment for the sensor inclination (equation (A1); Table A1). The effect of the adjustment on hourly CO_2 flux was small, with the slope of 1.6% and an offset of 0.016 mg CO_2 m^{-1} s^{-1}. (b) The uncorrected fluxes plotted versus those with adjusted surface heating correction. The effect of the adjusted heating correction on hourly CO_2 flux was still relatively small, with the slope 3% and an offset of 0.01 mg CO_2 m^{-1} s^{-1}. (c) Hourly fluxes before and after the correction plotted for the entire year.

correction, the fluxes became small but positive, suggesting small release of CO_2. Statistically, however, error bars crossed the zero in all corrected cases and resulted fluxes were not significantly different from zero. These results are also corroborated by the nearly constant and minimal rates of carbon exchange reported under similar conditions in other studies [*Zimov et al.*, 1993; *Elberling*, 2007]. At the same time, there was only one occurrence of a small negative daily correction (not significantly different from zero) at temperatures below 0°C (Figure A1b).

Figure A2 show the resulted hourly CO_2 fluxes throughout the entire year. The difference between the adjusted and the original corrections is illustrated in Figure A2a. The effect of the adjustment was small, with the slope of 1.016 and an offset of 0.016 mg CO_2 m^{-1} s^{-1}, with adjusted correction being slightly smaller in magnitude in comparison to the original one. The difference between the corrected and uncorrected fluxes is shown in Figure A2b. The effect was also small, with the slope of 1.03 and an offset of −0.01 mg CO_2 m^{-1} s^{-1}. The correction slightly reduced the uptakes and increased the released in comparison with uncorrected

values. The yearly patterns of the hourly fluxes are shown in Figure A2c before and after the heating correction, illustrating the small and consistent impact of the correction throughout the year, as expected at this primarily cold ecosystem.

The inclination adjustment presented above is a site-specific rough first approximation, and it employs significant empiricism and a number of assumptions, in addition to already significant assumptions employed in Method 4 (submethod: linear regression with air temperature; *Burba et al.*, 2008) for vertical sensor. While realizing these deficiencies, we unfortunately do not have a number of necessary parameters to get to a finer, more fundamental, adjustment model (e.g., measured instrument surface temperatures, incoming and outgoing long-wave radiation, and amounts of snow and ice on the instrument surfaces), which would have been a better and more reliable approach to a heating of the severely inclined open-path analyzer.

Acknowledgments

We would like to thank the North Slope Borough for support throughout this study. In addition, this paper was greatly improved with the useful comments of anonymous reviewers. The research described in this paper was performed under grants from National Science Foundation NSF OPP (ARC-1204263) and Department of Energy DOE TES program, and analysis was performed with funding from the Carbon in Arctic Reservoirs Vulnerability Experiment (CARVE), an Earth Ventures (EV-1) investigation, under contract with the National Aeronautics and Space Administration. Rommel Zulueta and Jospeph Verfaille were particularly helpful in establishing and conducting the research as was Doug Whiteman.

References

Arneth, A., J. Kurbatova, O. Kolle, O. B. Shibistova, J. Lloyd, N. N. Vygodskaya, and E. D. Schulze (2002), Comparative ecosystem-atmosphere exchange of energy and mass in a European Russian and a central Siberian bog II. Interseasonal and interannual variability of CO_2 fluxes, *Tellus Ser. B-Chem. Phys. Meteorol.*, *54*, 514–530.

Baldocchi, D. D., B. B. Hicks, and T. P. Meyers (1988), Measuring biosphere-atmosphere exchanges of biologically related gases with micrometeorological methods, *Ecology*, *69*, 1331–1340.

Baldocchi, D. D., et al. (2001), FLUXNET: A new tool to study the temporal and spatial variability of ecosystem-scale carbon dioxide, water vapor, and energy flux densities, *Bull. Am. Meteorol. Soc.*, *82*, 2415–2434.

Bate, G. C., and V. R. Smith (1983), Photosynthesis and respiration in the sub-Antarctic tussock grass poa-cookii, *New Phytol.*, *95*, 533–543.

Burba, G., D. McDermitt, A. Grelle, D. Anderson, and L. K. Xu (2008), Addressing the influence of instrument surface heat exchange on the measurements of CO_2 flux from open-path gas analyzers, *Global Change Biol.*, *14*, 1854–1876.

Clement, R., G. Burba, A. Grelle, D. Anderson, and J. Moncrieff (2009), Improved trace gas flux estimation through IRGA sampling optimization, *Agric. For. Meteorol.*, *149*, 623–638.

Corradi, C., O. Kolle, K. Walter, S. A. Zimov, and E. D. Schulze (2005), Carbon dioxide and methane exchange of a north-east Siberian tussock tundra, *Global Change Biol.*, *11*, 1910–1925.

Coyne, P. I., and J. J. Kelley (1971), Exchange of atmospheric carbon dioxide over an arctic tundra surface, *Trans., Am. Geophys. Union*, *52*, 842–853.

Davidson, E. A., and I. A. Janssens (2006), Temperature sensitivity of soil carbon decomposition and feedbacks to climate change, *Nature*, *440*, 165–173.

Elberling, B. (2007), Annual soil CO_2 effluxes in the high Arctic: The role of snow thickness and vegetation type, *Soil Biol. Biochem.*, *39*, 646–654.

Elberling, B., and K. K. Brandt (2003), Uncoupling of microbial CO_2 production and release in frozen soil and its implications for field studies of arctic C cycling, *Soil Biol. Biochem.*, *35*, 263–272.

Euskirchen, E. S., M. S. Bret-Harte, G. J. Scott, C. Edgar, and G. R. Shaver (2012), Seasonal patterns of carbon dioxide and water fluxes in three representative tundra ecosystems in northern Alaska, *Ecosphere*, *3*(1), 4.

Everett, K. R. (1980), Distribution and variability of soils near Atkasook, Alaska, *Arct. Antarct. Alp. Res.*, *12*, 433–446.

Fahnestock, J. T., M. H. Jones, P. D. Brooks, D. A. Walker, and J. M. Welker (1998), Winter and early spring CO_2 efflux from tundra communities of northern Alaska, *J. Geophys. Res.*, *103*, 29,023–29,027.

Fahnestock, J. T., M. H. Jones, and J. M. Welker (1999), Wintertime CO_2 efflux from arctic soils: Implications for annual carbon budgets, *Global Biogeochem. Cycles*, *13*, 775–779.

Fang, C., and J. B. Moncrieff (2001), The dependence of soil CO_2 efflux on temperature, *Soil Biol. Biochem.*, *33*, 155–165.

Falge, E., et al. (2001), Gap filling strategies for long term energy flux data sets, *Agric. For. Meteorol.*, *107*, 71–77.

Friborg, T., T. R. Christensen, and H. Sogaard (1997), Rapid response of greenhouse gas emission to early spring thaw in a subarctic mire as shown by micrometeorological techniques, *Geophys. Res. Lett.*, *24*, 3061–3064.

Gorham, E. (1991), Northern peatlands—Role in the carbon-cycle and probable responses to climatic warming, *Ecol. Appl.*, *1*, 182–195.

Grelle, A., and G. Burba (2007), Fine-wire thermometer to correct CO_2 fluxes by open-path analyzers for artificial density fluctuations, *Agric. For. Meteorol.*, *147*, 48–57.

Griffis, T. J., W. R. Rouse, and J. M. Waddington (2000), Scaling net ecosystem CO_2 exchange from the community to landscape-level at a subarctic fen, *Global Change Biol.*, *6*, 459–473.

Groendahl, L., T. Friborg, and H. Soegaard (2007), Temperature and snow-melt controls on interannual variability in carbon exchange in the high Arctic, *Theor. Appl. Climatol.*, *88*, 111–125.

Grogan, P., A. Michelsen, P. Ambus, and S. Jonasson (2004), Freeze-thaw regime effects on carbon and nitrogen dynamics in sub-arctic heath tundra mesocosms, *Soil Biol. Biochem.*, *36*, 641–654.

Harazono, Y., M. Mano, A. Miyata, R. C. Zulueta, and W. C. Oechel (2003), Inter-annual carbon dioxide uptake of a wet sedge tundra ecosystem in the Arctic, *Tellus Ser. B*, *55*, 215–231.

Hinzman, L. D., et al. (2005), Evidence and implications of recent climate change in northern Alaska and other arctic regions, *Clim. Change*, *72*, 251–298.

Hirata, R., et al. (2007), Seasonal and interannual variations in carbon dioxide exchange of a temperate larch forest, *Agric. For. Meteorol.*, *147*, 110–124.

Jarvi, L., I. Mammarella, and W. Eugster (2009), Comparison on net CO_2 fluxes measured with open- and closed-path infrared gas analyzers in urban complex environment, *Boreal Environ. Res.*, *14*, 499–514.

Kappen, L. (1993), Plant activity under snow and ice, with particular reference to lichens, *Arctic*, *46*, 297–302.

Komarkova, V., and P. J. Webber (1980), Two low Arctic vegetation maps near Atkasook, Alaska, *Arct. Antarct. Alp. Res.*, *12*, 447–472.

Kutzbach, L., et al. (2007), CO_2 flux determination by closed-chamber methods can be seriously biased by inappropriate application of linear regression, *Biogeosciences*, *4*, 1005–1025.

Kwon, H. J., W. C. Oechel, R. C. Zulueta, and S. J. Hastings (2006), Effects of climate variability on carbon sequestration among adjacent wet sedge tundra and moist tussock tundra ecosystems, *J. Geophys. Res.*, *111*, G03014, doi:10.1029/2005JG000036.

Laskowski, C. A. (2010), Spatial and temporal patterns of carbon exchange in the Alaskan Arctic tundra ecosystem, PhD dissertation in Ecology, San Diego State Univ., and the Univ. of Calif., Davis.
Laurila, T., H. Soegaard, C. R. Lloyd, M. Aurela, J. P. Tuovinen, and C. Nordstroem (2001), Seasonal variations of net CO_2 exchange in European Arctic ecosystems, *Theor. Appl. Climatol.*, *70*, 183–201.
Lee, X., W. J. Massman, and B. E. Law (2004), *Handbook of Micrometeorology: A Guide for Surface Flux Measurement and Analysis*, Kluwer Academic, Dordrecht; Boston; London.
Lee, H., E. A. G. Schuur, K. S. Inglett, M. Lavoie, and J. P. Chanton (2012), The rate of permafrost carbon release under aerobic and anaerobic conditions and its potential effects on climate, *Global Change Biol.*, *18*, 515–527.
Lund, M. J. M., J. M. Falk, T. Friborg, H. N. Mbufong, C. Sigsgaard, H. Soegaard, and M. P. Tamstorf (2012), Trends in CO_2 exchange in a high Arctic tundra heath, *J. Geophys. Res.*, *117*, G02001, doi:10.1029/2011JG001901.
Mahecha, M. D., et al. (2010), Global convergence in the temperature sensitivity of respiration at ecosystem level, *Science*, *329*, 838–840.
Marushchak, M. E., et al. (2013), Carbon dioxide balance of subarctic tundra from plot to regional scales, *Biogeosciences*, *10*, 437–452.
Massman, W., and J. Frank (2009), *Three Issues Concerning Open- and Closed-Path Sensors: Self-Heating, Pressure Effects, and Tube Wall Adsorption*, AsiaFlux Workshop, Sapporo, Japan, October 2009.
Mastepanov, M., S. Charlotte, E. J. Dlugokencky, H. Sander, S. Lena, P. T. Mikkel, and R. C. Torben (2008), Large tundra methane burst during onset of freezing, *Nature*, *456*, 628–630.
Mckane, R. B., E. B. Rastetter, G. R. Shaver, K. J. Nadelhoffer, A. E. Giblin, J. A. Laundre, and F. S. Chapin (1997), Climatic effects on tundra carbon storage inferred from experimental data and a model, *Ecology*, *78*, 1170–1187.
Michaelson, G. J., and C. L. Ping (2003), Soil organic carbon and CO_2 respiration at subzero temperature in soils of Arctic Alaska, *J. Geophys. Res.*, *108*(D2), 8164, doi:10.1029/2001JD000920.
Mikan, C. J., J. P. Schimel, and A. P. Doyle (2002), Temperature controls of microbial respiration in arctic tundra soils above and below freezing, *Soil Biol. Biochem.*, *34*, 1785–1795.
Moffat, A. M., et al. (2007), Comprehensive comparison of gap-filling techniques for eddy covariance net carbon fluxes, *Agric. For. Meteorol.*, *147*, 209–232.
Myneni, R. B., C. D. Keeling, C. J. Tucker, G. Asrar, and R. R. Nemani (1997), Increased plant growth in the northern high latitudes from 1981 to 1991, *Nature*, *368*, 698–702.
Natali, S. M., E. A. G. Schuur, K. S. Inglett, M. Lavoie, and J. P. Chanton (2012), Increased plant productivity in Alsakan tundra as a result of experimental warming of soil and permafrost, *J. Ecol.*, *100*, 488–498.
Oechel, W. C. (1976), Seasonal patterns of temperature response of CO_2 flux and acclimation in arctic mosses growing in situ, *Photosynthetica*, *10*, 447–456.
Oechel, W. C., W. T. Lawrence, J. Mustafa, and J. Martinez (1981), Energy and carbon acquisition, in *Resource Use by Chaparral and Matorral: A Comparison of Vegetation Function in Two Mediterranean-Type Ecosystems*, edited by P. C. Miller, pp. 151–183, Springer Verlag, New York and Heidelberg-Berlin.
Oechel, W. C., S. J. Hastings, G. L. Vourlitis, M. Jenkins, G. Riechers, and N. Grulke (1993), Recent change of Arctic tundra ecosystems from a net carbon-dioxide sink to a source, *Nature*, *361*, 520–523.
Oechel, W. C., G. L. Vourlitis, S. J. Hastings, and S. A. Bochkarev (1995), Change in arctic CO_2 flux over 2 decades—Effects of climate-change at barrow, Alaska, *Ecol. Appl.*, *5*, 846–855.
Oechel, W. C., G. Vourlitis, and S. J. Hastings (1997), Cold season CO_2 emission from arctic soils, *Global Biogeochem. Cycles*, *11*, 163–172.
Oechel, W. C., G. L. Vourlitis, S. J. Hastings, R. C. Zulueta, L. Hinzman, and D. Kane (2000), Acclimation of ecosystem CO_2 exchange in the Alaskan Arctic in response to decadal climate warming, *Nature*, *406*, 978–981.
Olsson, P. Q., M. Sturm, C. H. Racine, V. Romanovsky, and G. E. Liston (2003), Five stages of the Alaskan arctic cold season with ecosystem implications, *Arct. Antarct. Alp. Res.*, *25*, 74–81.
Panikov, N. S., P. W. Flanagan, W. C. Oechel, M. A. Mastepanov, and T. R. Christensen (2006), Microbial activity in soils frozen to below −39 degrees C, *Soil Biol. Biochem.*, *38*, 785–794.
Pries, C. E. H., E. A. G. Schuur, and G. Crummer (2013), Thawing permafrost increases old soil autotrophic respiration in tundra: Partitioning ecosystem respiration using δ13C and Δ14C, *Global Change Biol.*, *19*, 649–661.
Reichstein, M., et al. (2005), On the separation of net ecosystem exchange into assimilation and ecosystem respiration: Review and improved algorithm, *Global Change Biol.*, *11*, 1424–1439.
Reverter, B. R., et al. (2011), Adjustment of annual NEE and ET for the open-path IRGA self-heating correction: Magnitude and approximation over a range of climate, *Agric. For. Meteorol.*, *151*, 1856–1861.
Runkle, B. R. K., T. Sachs, C. Wille, E. M. Pfeiffer, and L. Kutzbach (2012), Bulk partitioning the growing season net ecosystem exchange of CO_2 in Siberian tundra reveals the seasonality of its carbon sequestration strength, *Biogeosci., Discuss*, *9*, 13,713–13,742.
Schuur, E. A. G., et al. (2008), Vulnerability of permafrost carbon to climate change, *BioScience*, *58*, 701–714.
Semikhatova, O. A. (1992), Relations between chloroplasts and mitochondria in the dark, *Sov. Plant Physiol.*, *39*, 391–395.
Starr, G., and S. F. Oberbauer (2003), Photosynthesis of arctic evergreens under snow: Implications for tundra ecosystem carbon balance, *Ecology*, *84*, 1415–1420.
Sturm, M., et al. (2005), Winter biological processes could help convert arctic tundra to shrubland, *BioScience*, *55*, 17–26.
Sullivan, P. F., J. M. Welker, S. J. T. Arens, and B. Sveinbjornsson (2008), Continuous estimates of CO_2 efflux from arctic and boreal soils during the snow-covered season in Alaska, *J. Geophys. Res.*, *113*, G04009, doi:10.1029/2008JG000715.
Sveinbjörnsson, B., and W. C. Oechel (1981), Controls on CO_2 exchange in two polytrichum moss species. 2. The implication of belowground plant parts on the whole-plant carbon balance, *Oikos*, *36*, 348–354.
Tarnocai, C., J. G. Canadell, E. A. G. Schuur, P. Kuhry, G. Mazhitova, and S. Zimov (2009), Soil organic carbon pools in the northern circumpolar permafrost region, *Global Biogeochem. Cycles*, *23*, GB2023, doi:10.1029/2008GB003327.
Trucco, C., E. A. G. Schuur, S. M. Natali, E. F. Belshe, R. Bracho, and J. Vogel (2012), Seven-year trends of CO_2 exchange in a tundra ecosystem affected by long-term permafrost thaw, *J. Geophys. Res.*, *117*, G02031, doi:10.1029/2011JG001907.
Walker, D. A., E. Binnian, B. M. Evans, N. D. Lederer, E. Nordstrand, and P. J. Webber (1989), Terrain, vegetation, and landscape evolution of the R4D research site, Brooks Range Foothills, Alaska, *Holarctic Ecol.*, *12*, 238–261.
Walton, D. W. H., and C. S. M. Doake (1987), *Antarctic Science*, Cambridge Univ. Press, Cambridge, New York.
Wang, X., S. Piao, P. Ciais, I. A. Janssens, M. Reichstein, S. Peng, and T. Wang (2010), Are ecological gradients in seasonal Q_{10} of soil respiration explained by climate or by vegetation seasonality?, *Soil Biol. Biochem.*, *42*, 1728–1734.
Webb, E. K., G. I. Pearman, and R. Leuning (1980), Correction of flux measurements for density effects due to heat and water-vapor transfer, *Q. J. R. Meteorol. Soc.*, *106*, 85–100.

Welker, J. M., J. T. Fahnestock, and M. H. Jones (2000), Annual CO_2 flux in dry and moist arctic tundra: Field responses to increases in summer temperatures and winter snow depth, *Clim. Change*, *44*, 139–150.
Weller, G., and B. Holmgren (1974), Microclimates of Arctic tundra, *J. Appl. Meteorol.*, *13*, 854–862.
Wilson, K., et al. (2002), Energy balance closure at FLUXNET sites, *Agric. For. Meteorol.*, *113*, 223–243.
Zamolodchikov, D. G., and D. V. Karelin (2001), An empirical model of carbon fluxes in Russian tundra, *Global Change Biol.*, *7*, 147–161.
Zimov, S. A., et al. (1993), Winter biotic activity and production of CO_2 in Siberian soils—A factor in the greenhouse effect, *J. Geophys. Res.*, *98*, 5017–5023.
Zimov, S. A., S. P. Davidov, Y. V. Voropaev, S. F. Prosiannikov, I. P. Semiletov, M. C. Chapin, and F. S. Chapin (1996), Siberian CO_2 efflux in winter as a CO_2 source and cause of seasonality in atmospheric CO_2, *Clim. Change*, *33*, 111–120.
Zimov, N. S., S. A. Zimov, A. E. Zimova, G. M. Zimova, V. I. Chuprynin, and F. S. Chapin (2009), Carbon storage in permafrost and soils of the mammoth tundra-steppe biome: Role in the global carbon budget, *Geophys. Res. Lett.*, *36*, L02502, doi:10.1029/2008GL036332.
Zona, D., et al. (2009), Methane fluxes during the initiation of a large-scale water table manipulation experiment in the Alaskan Arctic tundra, *Global Biogeochem. Cycles*, *23*, GB2013, doi:10.1029/2009GB003487.
Zona, D., D. A. Lipson, R. C. Zulueta, S. F. Oberbauer, and W. C. Oechel (2011), Microtopographic controls on ecosystem functioning in the Arctic coastal plain, *J. Geophys. Res.*, *116*, G00I08, doi:10.1029/2009JG001241.